Electronic Supplementary Material (ESI) for Nanoscale.
This journal is © The Royal Society of Chemistry 2018

Supporting Information for:

Controlling the Phase Transition in Nanocrystalline Ferroelectric Thin Films via Cation Ratio

Iryna S. Golovina[1], Matthias Falmbigl[1], Christopher J. Hawley[1,2], Anthony Ruffino[1], Aleksandr V. Plokhikh[1], Igor A. Karateev[3], Thomas C. Parker[4], Alejandro Gutierrez-Perez[1], Alexandre L. Vasiliev[4], and Jonathan E. Spanier[*1,5,6]

[1]*Department of Materials Science & Engineering, Drexel University, Philadelphia, Pennsylvania 19104, USA*

[2]*Department of Physics, Lafayette College, Easton PA 18042, USA*

[3]*National Research Center "Kurchatov Institute", Kurchatov Square 1, Moscow 123182, Russia*

[4]*US Army Research Laboratory, Aberdeen Proving Ground, Maryland 21005, USA*

[5]*Department of Electrical & Computer Engineering, Drexel University, Philadelphia, Pennsylvania 19104, USA*

[6]*Department of Physics, Drexel University, Philadelphia, Pennsylvania 19104, USA*

Grain sizes

The distribution of grain sizes was obtained from the TEM images for four samples with various Ba/Ti ratios. All evaluated samples had *top Pt electrodes* deposited *before* the annealing step. **Figure S1** shows the distribution for each sample. The solid red curves are the histogram fitting by a Gaussian function. The mean values and standard deviations obtained from the fitting for each composition are as follows (in nm): 8.066 ± 0.643, 11.970 ± 0.694, 12.094 ± 0.481, and 8.697 ± 0.344 for films with Ba/Ti-ratio equals 0.8, 0.92, 1.01, and 1.06, respectively. In addition, TEM images for a stoichiometric sample (Ba/Ti=1.01) with *top Pt electrodes* deposited *after* the annealing step have been analyzed. The distribution of grain sizes for this sample is presented in **Figure S2**.

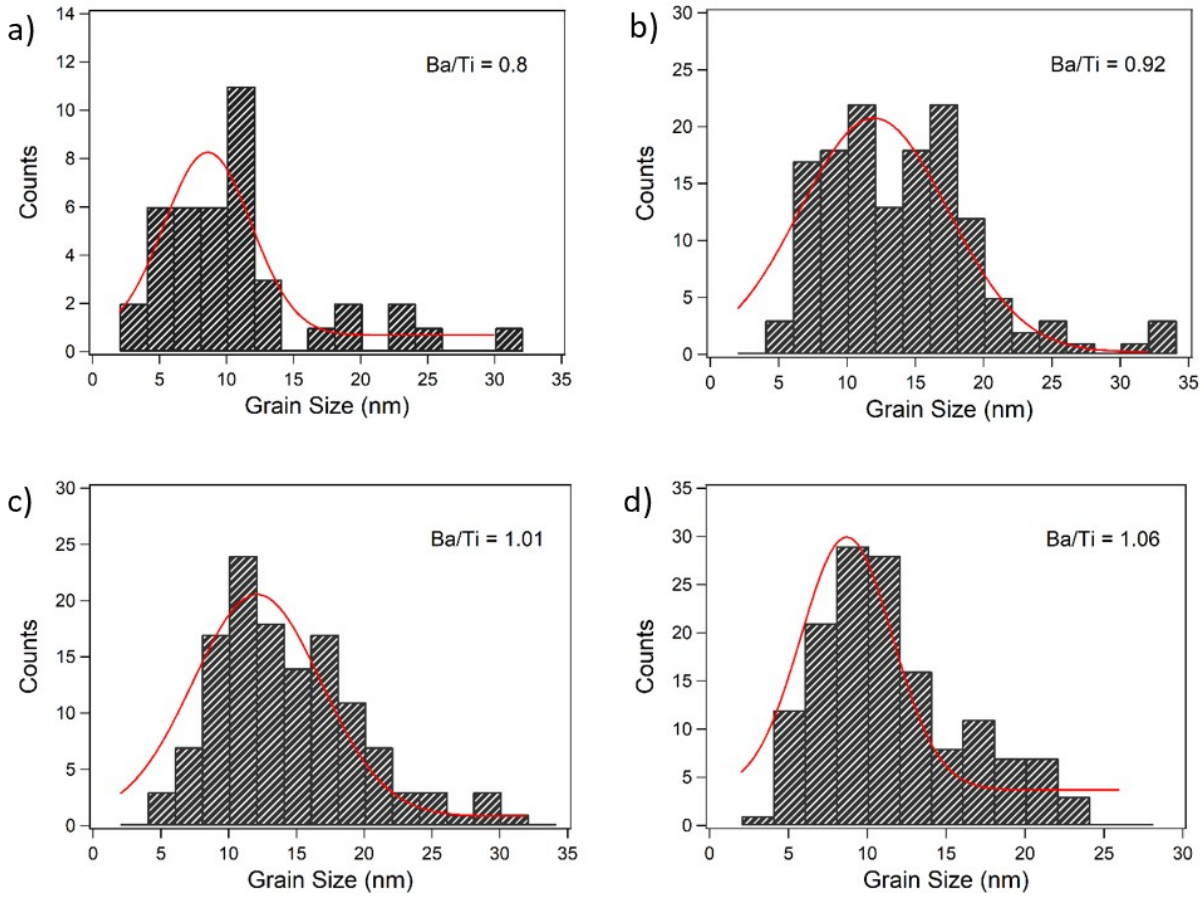

Figure S1. The distribution of grain sizes *beneath top Pt electrodes* deposited *before* annealing step for samples with various Ba/Ti ratios: a) 0.8, b) 0.92, c) 1.01, d) 1.06. Solid red curves are fits to the histogram using a Gaussian.

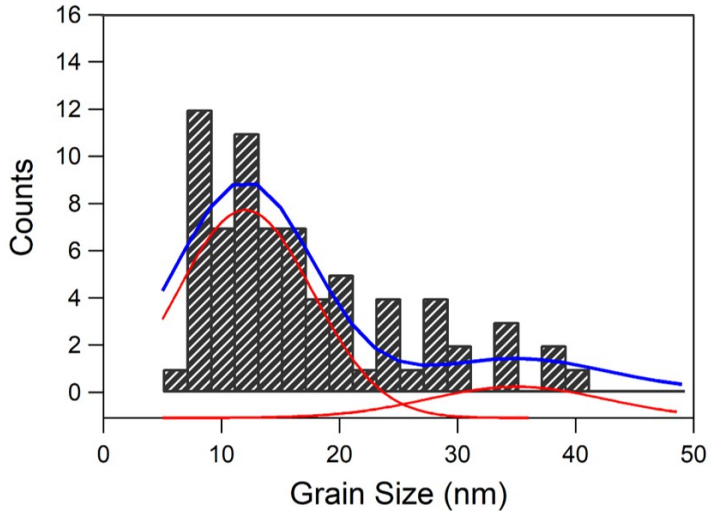

Figure S2. The distribution of grain sizes *beneath top Pt electrodes* deposited *after* the annealing step for a stoichiometric sample (Ba/Ti=1.01). Red curves are two Gaussian functions and the blue curve is the sum of these fit functions to the histogram.

A TEM cross section beneath uncovered area (between top electrodes) was also examined in a similar way. The distribution of grain sizes obtained from this area and the histogram fitting by a Gaussian function are depicted in **Figure S3**. The mean value and standard deviation obtained from the fitting is 17.067 ± 0.765 nm.

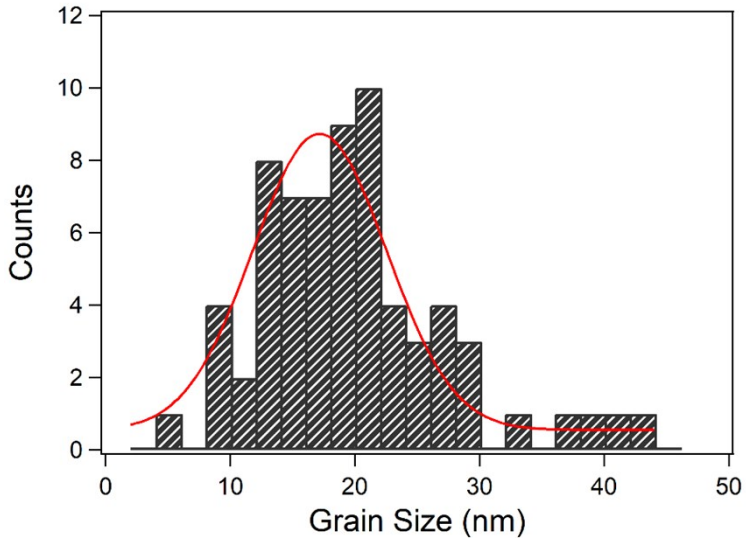

Figure S3. Grain size distribution from the TEM cross section between the uncovered area (between top electrodes) obtained for a stoichiometric sample (Ba/Ti=1.01). Solid red curve is the histogram fitting by a Gaussian function.

XPS data

The XPS Ti spectra for the films with Ba/Ti ratio of 0.8, 0.92, 1.01 and 1.06 and corresponding fits are presented in **Fig. S4a**. The two peaks at 458.21 eV and 464 eV originate from the Ti2p3/2 and Ti2p1/2 lines, respectively, and do not shift in energy as a function of composition. The Ti2p3/2 peak is fitted by one Voigt (Gaussian/Lorentzian=50/50) function at 458.19 eV (**Fig. S4b**), which corresponds to the valence state of Ti^{4+}. The FWHM of the Ti2p3/2 peak is 1.15 eV in all cases.

The XPS Ba spectra for the films with Ba/Ti=0.8, 0.92, 1.01 and 1.06 are displayed in **Fig. S5a**. The small shift of the Ba spectra is in the range of instrumental error, when we take the C1s lines as a standard for a linear calibration. The Ba3d5/2 spectrum contains two maxima. The

Ba3d5/2 peak for the film with Ba/Ti=1.06 is fitted by two Voigt (Gaussian/Lorentzian=50/50) functions: at 778.84 eV and 780.24 eV, the FWHM of which are 1.3 eV and 1.63 eV, respectively (**Fig. S5b**). The peak at lower binding energy originates from the barium in deeper layers, and the peak at higher binding energy from the barium on the surface that could arise due to residual unavoidable amount of $BaCO_3$ or $Ba(OH)_2$. The intensity of the line of the barium in deeper layers monotonically increases, while the intensity of the line corresponding to the barium on the surface systematically decreases with increasing Ba/Ti ratio.

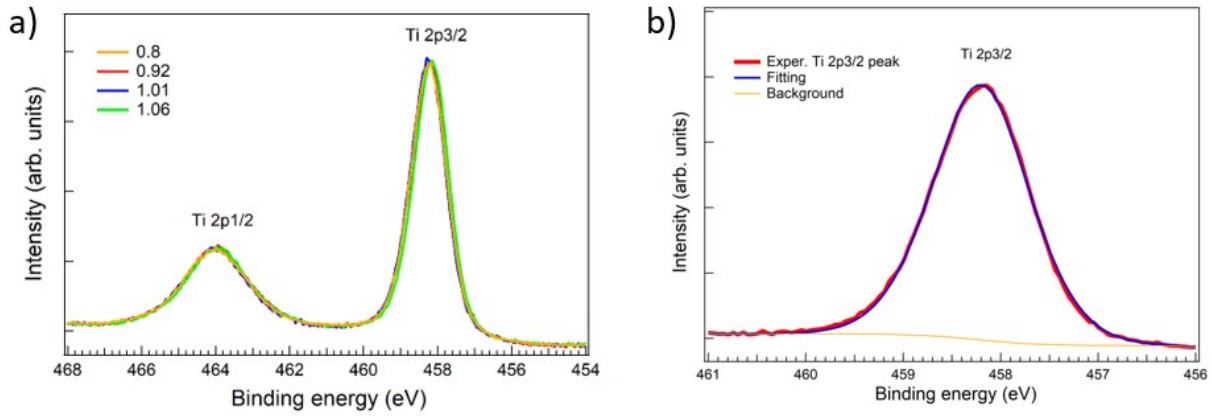

Figure S4. The experimental XPS Ti spectra collected for the films with Ba/Ti=0.8, 0.92, 1.01, 1.06 (a) and fitting of the experimental Ti 2p3/2 peak by a Voigt function.

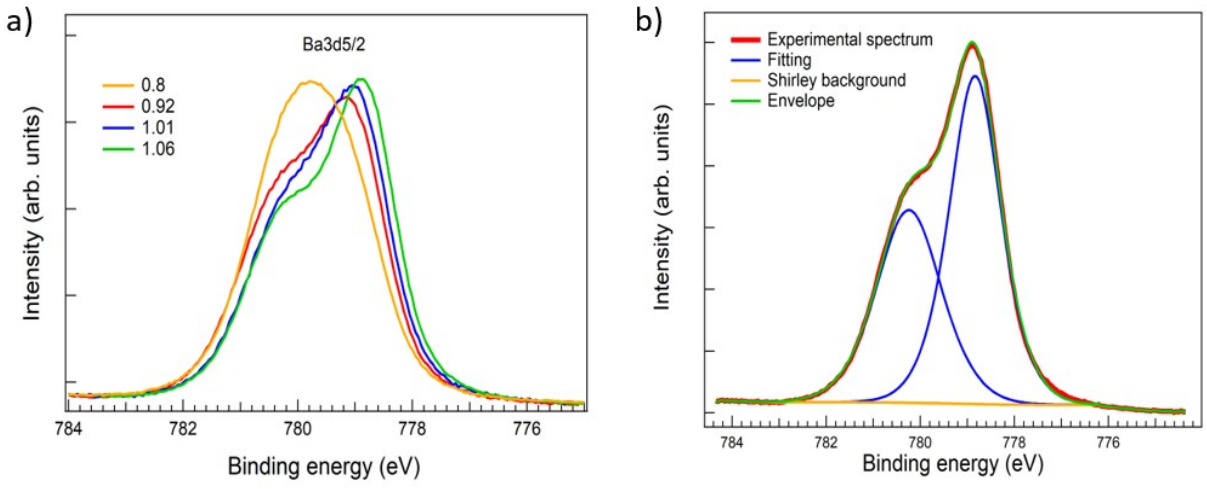

Figure S5. The experimental XPS Ba spectra collected for the films with Ba/Ti=0.8, 0.92, 1.01, 1.06 (a) and fitting of the experimental Ba 3d5/2 spectrum for the film with Ba/Ti=1.06 by a Voigt function.

Electrical data

Figure S6 shows the electric field dependence of current density and frequency dependence of dielectric constant for all films studied. The data have been collected at room temperature. Fig. S6a demonstrates that the films with different stoichiometry with *top Pt electrodes* deposited *before* the annealing step are basically identical in their J-E response. However, the stoichiometric film (Ba/Ti=1.01) with *Pt electrodes* deposited *after* annealing experiences higher leakage current than the stoichiometric film with *electrodes* deposited *before* annealing. The error bars in Fig. S6b were evaluated using 5 independently collected data sets for each MIM-capacitor. Considering the films with *Pt electrodes* deposited *before* the annealing step, one can state that the room temperature dielectric constant strongly depends on stoichiometry, especially on the Ti-rich side. It is reduced by 50% in the Ti-rich samples compared to the stoichiometric one (Ba/Ti=1.01), but remains almost unchanged upon further increasing the Ba/Ti ratio. It should also be noted that dielectric constant is ~110 for the stoichiometric film (Ba/Ti=1.01) with *top Pt electrodes* deposited *after* the annealing procedure, and this is significantly lower than the dielectric constant ~160 for the film with *Pt electrodes* deposited *before* annealing.

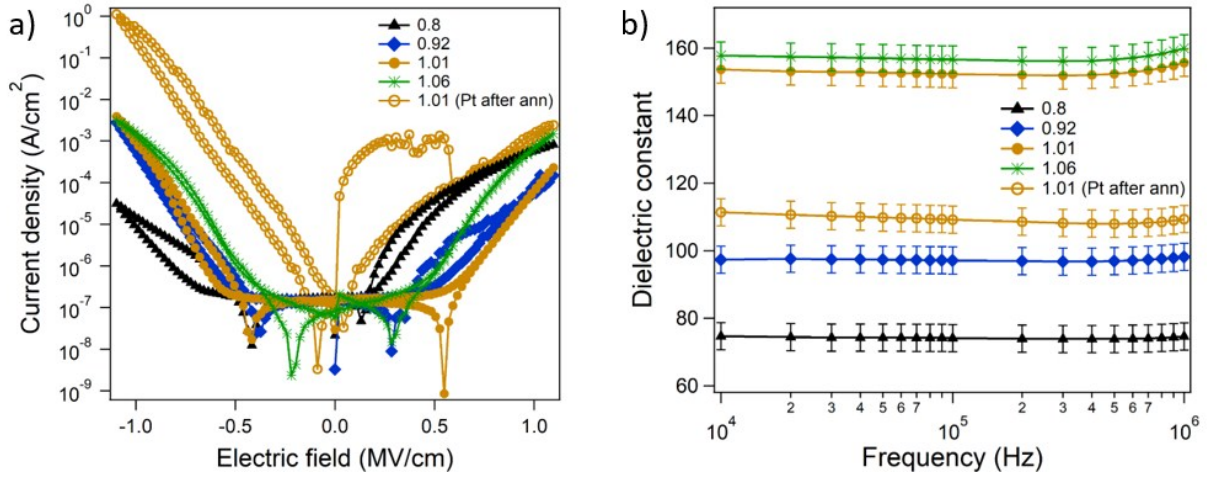

Figure S6. Room temperature current density as a function of electric field (a) and dielectric constant as a function of frequency (b) for the films with Ba/Ti=0.8, 0.92, 1.01 and 1.06.

Polarization loops

Figures S7 and S8 represent room temperature hysteresis loops collected for the stoichiometric (Ba/Ti=1.01) film with *Pt electrodes* deposited *after* the annealing step. The hysteresis loops were measured at different maximum electric fields and different measuring frequencies. The hysteresis loop measured at a maximum electric field of 0.65 MV/cm and a frequency of 1 kHz exhibits a maximum polarization of 7.5 μC/cm^2, while the influence of the leakage current is negligible there. This representative hysteresis loop is shown in Figure 6 in the main paper and is used for the analysis.

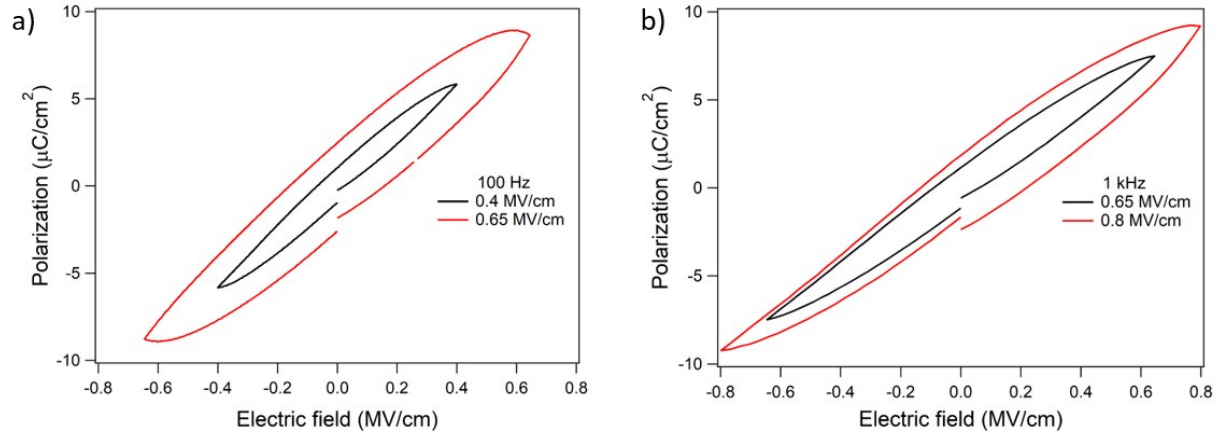

Figure S7. Room temperature hysteresis loops collected at different maximum electric fields and different frequencies for the stoichiometric (Ba/Ti=1.01) film with *Pt electrodes* deposited *after* the annealing procedure.

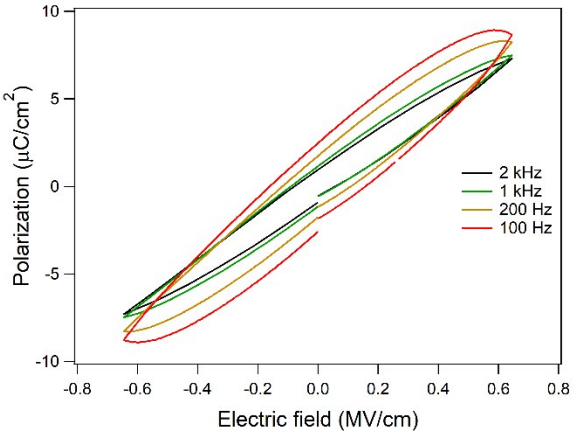

Figure S8. Room temperature hysteresis loops collected at a maximum electric field of 0.65 MV/cm and at different frequencies for the stoichiometric (Ba/Ti=1.01) film with *Pt electrodes* deposited *after* the annealing procedure.

Raman spectra

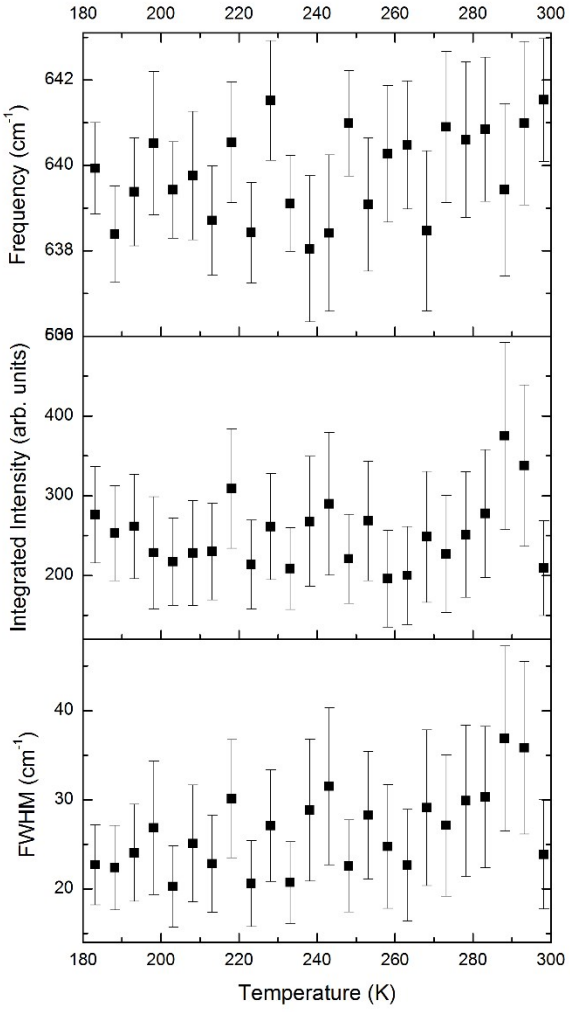

Figure S9. Temperature dependences of the integrated intensity, frequency, and FWHM of the Raman mode at 620 cm^{-1} for the Ti-rich sample (Ba/Ti=0.8).